



QUANTUM CHEMICAL STUDY TO INVESTIGATE THE EFFECTS OF 5'-3' DIPHOSPHATE BACKBONE ON THE CONFORMATION OF HYPERMODIFIED NUCLEOTIDE LYSIDINE (K²C) OCCUR AT WOBBLE (34TH) POSITION IN THE ANTICODON LOOP OF tRNA^{ILE}

SONAWANE K.D.^{1*}, KUMBHAR B.V.¹, KUMBHAR N.M.², SAMBHARE S.B.¹, KAMBLE A.D.¹ AND BAVI R.S.¹

¹Structural Bioinformatics Unit, Department of Biochemistry, Shivaji University, Kolhapur, 416 004, MS, India

²Department of Biotechnology, Shivaji University, Kolhapur, 416 004, MS, India

*Corresponding author. E-mail: kds_biochem@unishivaji.ac.in, kds19@rediffmail.com, Phone: +91 9881320719

Received: January 27, 2011; Accepted: February 08, 2011

Short Title: Diphosphate lysidine nucleotide

Abstract- Conformational preferences of hypermodified nucleotide 'lysidine' in the model diphosphate (Me-p-k²C-p-Me) segment of anticodon loop of tRNA^{ile} have been studied by using quantum chemical perturbative configuration interaction with localized orbitals (PCILO) method. The consequences of 5'-3' diphosphate backbone on the conformation of zwitterionic, non-zwitterionic, neutral and tautomeric forms of lysidine have been investigated and compared with diphosphate backbone of cytidine nucleotide. Automated geometry optimization using semi-empirical quantum chemical RM1, quantum mechanical Hartree-Fock (HF-SCF) and Density Functional Theory (B3LYP/6-31G**) calculations have also been made to compare the salient features. The orientation of lysine moiety is found *trans* to the N(1) of cytidine in the predicted most stable conformations of all the four forms of lysidine in the model 5'-3' diphosphate anticodon loop segment. The lysine substituent folds back and form hydrogen bond with 2'-hydroxyl group of ribose sugar. Lysine substituent of various diphosphate lysidine nucleotides does not interact with 5' or 3' diphosphate backbone. All forms of lysidine nucleotides retain anti ($\chi=33^\circ$) glycosyl (glycosidic) torsion angle. Diphosphate cytidine nucleotide prefers ($\chi=33^\circ$), which could destabilize the c3'-*endo* sugar to the minor extent. The interaction between O(12b)---HO2' of tautomer diphosphate nucleotide may help in maintaining the c3'-*endo* sugar puckering at wobble (34th) position as compared to other lysidine forms and cytidine nucleotide. Hence, tautomeric form of lysidine along with suitable hydrogen bond donor-acceptor groups may also provide structural stability for the proper recognition of AUA codons instead of AUG codons.

Keywords: Hypermodified nucleotide, tRNA, lysidine (k²C), PCILO, DFT, 5'-3' diphosphate backbone.

Introduction

Transfer RNA is the most extensively modified nucleic acid in the cell, and immediately after its discovery it was shown that it contains modified nucleosides [1-2]. These modified nucleosides are present at 34th 'wobble' position and at 3' adjacent (37th) position in the anticodon loop of tRNA from all domains of life [3-5]. The modifications present at 3'-adjacent position prevent extended Watson-Crick base pairing during protein biosynthesis process, whereas the modifications present at 34th position may restrict or enlarge the scope of wobble base pairing [6-8]. Hypermodified nucleoside lysidine (k²C) occur at 34th 'wobble' position in the anticodon loop of *E.coli* tRNA^{ile}₂, *Bacillus subtilis*, *Mycoplasma capricolum* tRNA^{ile}, potato mitochondrial tRNA^{ile} and tRNA^{ile} of *Haloflex volcani* [9-14]. The substitution of the oxygen atom in position 2 of cytidine with ϵ -nitrogen atom of L-

lysine results in formation of lysidine. The condensation of lysine amino acid to the pyrimidine ring of cytidine leads to the modification of cytidine to lysidine. The lysidine modification prevents misrecognition of AUG as isoleucine and that of AUA as methionine [15]. The k²C modification also changes the aminoacylation identity of the tRNA from methionine to isoleucine [16]. The synthesis of lysidine in the precursor tRNA^{ile} by enzyme tRNA^{ile}-lysidine synthetase (*Tils*) has been reported in the *E.coli* and *Bacillus subtilis* [17]. Identification and characterization of tRNA^{ile}-lysidine synthetase (*Tils*) done by using lysine and ATP as a substrates [18]. NMR spectroscopy, mass spectroscopy and chemical analysis techniques are used to determine the chemical structure of modified nucleoside lysidine [19]. Structural basis for the mechanism of lysidine formation and translational fidelity by

tRNA^{le}-lysine synthetase (*Tls*) has also been carried out by mutant analysis, mass spectroscopy and X-ray crystallography methods [20-22]. Recently a polyamine-conjugated modified nucleoside (agmatidine or agm²C) has been identified at the wobble position of the archael tRNA^{le} which can also decode AUA codons similar to lysidine [23].

Several theoretical studies have been carried out to understand the structural significance of hypermodified nucleic acid bases, N⁶-(Δ^2 -isopentenyl) adenine, i⁶Ade, 2-methylthio-N⁶-(Δ^2 -isopentenyl) adenine, ms²ⁱ⁶Ade, N⁶-(Δ^2 -*cis*-hydroxyisopentenyl) adenine, *cis*-io⁶Ade, 2-methylthio-N⁶-(Δ^2 -*cis*-hydroxyisopentenyl) adenine, *cis*-ms²ⁱ⁶Ade, N⁶-(Δ^2 -*trans*-hydroxyisopentenyl) adenine, *trans*-io⁶Ade, 2-methylthio-N⁶-(Δ^2 -*trans*-hydroxyisopentenyl) adenine, *trans*-ms²ⁱ⁶Ade, N⁶-(N-threonylcarbamoyl) adenine, t⁶Ade, 2-methylthio-N⁶-(N-threonylcarbamoyl) adenine, ms^{2t6}Ade, N⁶-(N-glycylcarbamoyl) adenine, g⁶Ade and protonation induced conformational changes of these hypermodified bases occur at 37th position in the anticodon loop of tRNA [24-30]. Likewise, conformational preferences of modified nucleoside lysidine [31], queuosine 5'monophosphate 'pQ' and its protonated form 'pQH⁺' which present at 34th 'wobble' position have also been investigated theoretically [32]. Similarly, attempts have been made to find out the effect of ribose phosphate backbone on the conformation of other polynucleotides [33-41]. The stacking interactions of several dinucleoside monophosphate with and without hypermodified bases have been compared by using ultraviolet adsorption, circular dichroism (CD) and high resolution proton magnetic resonance [42]. The influence of the phosphodiester linkage on the conformation of the dinucleoside monophosphates has also been reported [43]. Earlier theoretical studies have been carried out to understand the conformational preferences of isolated modified nucleic acid bases [24-30], but very little is known about the consequences of ribose phosphate backbone on the conformation of these modified bases, except queuosine 5'monophosphate 'pQ' and its protonated form 'pQH⁺' [32].

Present study is an extension of earlier work [31] to investigate the conformational preferences of zwitterionic, non-zwitterionic, neutral, and tautomeric forms of hypermodified nucleotide lysidine in presence of 5'-3' diphosphate backbone of anticodon loop segment of tRNA^{le}. Conformational analysis of the ribose sugar ring puckering of all the lysidine forms and cytidine nucleotide have also been investigated by calculating the phase angle of pseudorotation (*P*) and amplitude (*Tm*). Earlier study on the conformational preferences of lysidine in absence of diphosphate backbone have shown that the lysine

moiety of all lysidine forms folds back and interacts with the 2'-hydroxyl group of ribose sugar [31] so that Watson-Crick hydrogen base pairing sites remain accessible to recognize AUA codons. Thus it is of interest to find out whether the orientation of lysine substituent prefers to interact with 5' or 3' phosphate backbone or it remains same as predicted earlier [31].

Nomenclature, Convention and Procedure:

Figure 1 show the atom numbering and identification of the various torsion angles specifying the internal rotation around the various acyclic chemical bonds for the model 5'-3' diphosphate nucleotide segment (Me-p-k²C-p-Me) of lysidine. The torsion angle α [N(1)C(2)N(2)C(7)] describes the rotation of C(7) around bond C(2)N(2) and measures the orientation of the bond N(2)C(7) with respect to the N(1)C(2) from the eclipsed position in the right hand sense of rotation. Likewise, the successive chemical bonds along the main extension of the lysine substituent define the subsequent torsion angles β , γ , δ , Ψ , ϕ , ξ , θ and η . Ribose - phosphate backbone torsion angles are distinguished by the subscript 'b' to refer to the backbone torsion angle along with respective anticodon base position in tRNA model [44]. Similarly, phosphate atoms of 34th and 35th nucleotide backbone are named P₍₃₄₎ and P₍₃₅₎ to differentiate between backbone torsion angles of respective nucleotide. Nomenclature and the torsion angle values of the diphosphate nucleotide backbone retain as specified for the 34th and 35th nucleotide position in the tRNA model [44] referring likewise to the right hand sense of rotation around the central bond, measured from the eclipsed position of the outer bonds $\zeta_{b(33)}$ [H-C3'-O3'-P₍₃₄₎], $\alpha_{b(34)}$ [C3'-O3'-P₍₃₄₎-O5'], $\beta_{b(34)}$ [O3'-P₍₃₄₎-O5'-C5'], $\gamma_{b(34)}$ [P₍₃₄₎-O5'-C5'-C4'], $\delta_{b(34)}$ [O5'-C5'-C4'-C3'], $\epsilon_{b(34)}$ [C5'-C4'-C3'-O3'], $\zeta_{b(34)}$ [C4'-C3'-O3'-P₍₃₅₎], $\alpha_{b(35)}$ [C3'-O3'-P₍₃₅₎-O5'], $\beta_{b(35)}$ [O3'-P₍₃₅₎-O5'-C5'], $\gamma_{b(35)}$ [P₍₃₅₎-O3'-C5'-H], χ [O1'-C1'-N(1)-C(6)] and the ribose ring torsion angles are τ_1 (C4'-O1'-C1'-C2'), τ_2 (O1'-C1'-C2'-C3'), τ_3 (C1'-C2'-C3'-C4'), τ_4 (C2'-C3'-C4'-O1'), τ_5 (C3'-C4'-O1'-C1'). For all the diphosphate models considered in this study, the glycosyl torsion angle orientation is held anti ($\chi=3^\circ$) and ribose ring puckering is c3'-*endo* as like 34th 'wobble' nucleotide, whereas 5'-3'diphosphate backbone torsion angles are held similar to 34th and 35th nucleotides as in Holbrook tRNA^{Phe} crystal structure [44]. Phosphate backbone at 5' and 3' side has been terminated by -CH₃ groups and one hydrogen atom is added to the oxygen (O1P) atom of phosphate (PO₄⁻) group to neutralize the phosphate backbone similarly as shown in earlier study [32].

For all the energy calculations of the different molecular conformations the quantum chemical perturbative configuration interaction with localized

orbitals PCILO method [45-47] has been utilized. PCILO method has been found to be widely useful, in conformational studies of several of bio-organic molecules, including nucleic acid constituents, analogs and peptide nucleic acid (PNA) [48-50]. For each conformation polarity of the chemical bonds has been optimized and correction terms up to the third order are retained in the calculation of the total ground state energy. In the multidimensional conformational space the logical selection of grid points approach is used for searching the most stable structure and the alternative stable structure [51]. Conformational energy calculations are started by appropriately selected bond lengths, bond angles and torsion angle values of lysine substituent from various forms of lysidine molecule [31] whereas, observed values are considered for the ribose phosphate backbone as given in the crystal structure [44]. Throughout the conformational search done by PCILO method the phosphate backbone torsion angles are not allowed to change freely so retained as in crystal structure [44]. The automated full geometry optimization calculations are carried out by using semi-empirical quantum chemical method RM1 [52], *ab-initio* molecular orbital Hartree-Fock (HF-SCF) quantum mechanical method using STO-3G basis set and Density Functional Theory using B3LYP/6-31G** [53, 54] basis set to compare salient features. These methods (RM1, HF-SCF and DFT) are implemented in commercially available PC Spartan Pro (version 6.1.1.0, Wavefunction Inc.) software [55]. During all the full geometry optimization calculations whole lysidine diphosphate nucleotides are allowed to optimize. The amplitude (T_m) and the phase angle pseudorotation (P) have been calculated according to the equations given in [56]. Thus, with the help of methods and procedure discussed above the consequences of 5' or 3' phosphate backbone on zwitterionic, non-zwitterionic, neutral and tautomer forms of lysidine incorporated in the diphosphate nucleotide anticodon loop segment of tRNA^{le} have been carried out.

Results and Discussion

Diphosphate zwitterionic form of lysidine

The PCILO predicted most stable structure of 5'-3' diphosphate hypermodified nucleotide segment (Me-p-k²C_(zwitter)-p-Me) of zwitterionic form of lysidine is depicted in Figure 2. The preferred torsion angle values describing the orientation of lysine substituent in the model nucleotide diphosphate segment are

($\alpha=180^\circ$, $\beta=180^\circ$, $\gamma=30^\circ$, $\delta=60^\circ$, $\psi=180^\circ$, $\varphi=60^\circ$, $\xi=330^\circ$, $\theta=150^\circ$, $\chi=3^\circ$). The positive charge is present on the N(1) of cytidine as well as at N(11) of lysine substituent and the negative charge is present on the carboxyl group of zwitterionic form of lysidine diphosphate molecule.

The lysine moiety of zwitterionic form of hypermodified nucleotide lysidine folds back towards the ribose sugar in presence of 5'-3' diphosphate segment of anticodon loop of tRNA. The carboxyl oxygen O(12a) of lysine substituent interacts with 2'-hydroxyl group of ribose sugar, along with HN(2), and HC(9) of lysine moiety. The carboxyl and amino groups of lysine substituent of zwitterion diphosphate nucleotide (Fig. 2) does not interact with 5' or 3' phosphate (PO₄⁻) groups. The preferred structure is stabilized by the intramolecular interactions between O(12a)---HO2', O(12a)---HN(2), O(12a)---HC(9), O(12b)---HN(11), and N(2)---HC(9) as shown in (Table 1). The orientation of lysine substituent is found *trans* to the N(1) of cytidine even in presence of ribose-phosphate backbone and may be compared with the zwitterionic form of lysidine in absence of phosphate backbone [31]. Allowing glycosyl torsion angle χ to change freely over the entire range (0 to 360°) retains original value ($\chi=3^\circ$). The conformation is stabilized by hydrogen bonding interactions (Table 1) between O5'---HC(6) and O1'---HC(6). The atom HC(6) of zwitterionic form of lysidine involved in bifurcating hydrogen bonding with O5' and O1' of phosphate backbone (Fig. 2). In addition of this the hydrogen bonding between O1P_{b(35)}---HC3' may provide additional stabilizing factor to the structure (Fig. 2).

Starting from the PCILO preferred conformation (Fig. 2) the full geometry optimization carried out by using semi-empirical quantum chemical (RM1) method results in torsion angles ($\alpha=181^\circ$, $\beta=164^\circ$, $\gamma=53^\circ$, $\delta=57^\circ$, $\psi=190^\circ$, $\varphi=78^\circ$, $\xi=88^\circ$, $\theta=161^\circ$,

$\chi=2^\circ$, $\zeta_{b(33)}=215^\circ$, $\alpha_{b(34)}=256^\circ$, $\beta_{b(34)}=129^\circ$, $\gamma_{b(34)}=187^\circ$, $\delta_{b(34)}=47^\circ$, $\epsilon_{b(34)}=94^\circ$, $\zeta_{b(34)}=220^\circ$, $\alpha_{b(35)}=322^\circ$, $\beta_{b(35)}=208^\circ$, $\gamma_{b(35)}=135^\circ$). The torsion angle values for β , γ , δ , ψ , φ , θ and χ slightly differ from the PCILO preferred values. The phosphate backbone torsion angles show close proximity with the crystal structure values [44] except torsion angles $\gamma_{b(34)}$ and $\zeta_{b(34)}$ vary by 30° whereas torsion angles $\alpha_{b(34)}$, $\beta_{b(34)}$ and $\alpha_{b(35)}$ change within 50°. The full geometry optimization of the PCILO preferred structure (Fig. 2) carried out by using HF-SCF (STO-3G) method results in torsion angles ($\alpha=173^\circ$, $\beta=85^\circ$, $\gamma=53^\circ$, $\delta=65^\circ$, $\psi=210^\circ$,

$\varphi=74^\circ$, $\xi=330^\circ$, $\theta=149^\circ$, $\chi=30^\circ$, $\zeta_{b(33)}=190^\circ$, $\alpha_{b(34)}=254^\circ$, $\beta_{b(34)}=171^\circ$, $\gamma_{b(34)}=187^\circ$, $\delta_{b(34)}=57^\circ$, $\epsilon_{b(34)}=92^\circ$, $\zeta_{b(34)}=199^\circ$, $\alpha_{b(35)}=308^\circ$, $\beta_{b(35)}=258^\circ$, $\gamma_{b(35)}=194^\circ$). The torsion angles α , δ , φ , χ , $\zeta_{b(34)}$, $\epsilon_{b(34)}$ and $\gamma_{b(35)}$ show minor differences from that of most stable PCILO preferred structure (Fig. 2). The torsion angles γ , ψ , $\gamma_{b(34)}$ and $\delta_{b(34)}$ changes by about 30° whereas large variations found in torsion angles β , $\alpha_{b(34)}$, $\alpha_{b(35)}$ and $\beta_{b(35)}$. The full

geometry optimization using the DFT (B3LYP/6-31G**) method results in torsion angles ($\alpha=172^\circ$, $\beta=86^\circ$, $\gamma=57^\circ$, $\delta=67^\circ$, $\psi=207^\circ$, $\phi=77^\circ$, $\xi=325^\circ$, $\theta=151^\circ$, $\chi=19^\circ$, $\zeta_{b(33)}=189^\circ$, $\alpha_{b(34)}=281^\circ$, $\beta_{b(34)}=140^\circ$, $\gamma_{b(34)}=149^\circ$, $\delta_{b(34)}=50^\circ$, $\epsilon_{b(34)}=77^\circ$, $\zeta_{b(34)}=184^\circ$, $\alpha_{b(35)}=286^\circ$, $\beta_{b(35)}=285^\circ$, $\gamma_{b(35)}=183^\circ$). The torsion angles α , δ , ξ , θ , $\zeta_{b(33)}$, and $\gamma_{b(35)}$ show minor variations from the PCILO preferred values (Fig. 2) whereas, the torsion angle ϕ , χ , $\alpha_{b(34)}$, $\gamma_{b(34)}$, $\delta_{b(34)}$, $\epsilon_{b(34)}$, $\zeta_{b(34)}$, and $\alpha_{b(35)}$ change by about 20° . The torsion angle γ , ψ , and $\beta_{b(34)}$ changes by about 30° . Other torsion angles β and $\beta_{b(35)}$ change by large difference. Results of geometrical parameters (Table 4) after the optimization by RM1, HF-SCF and DFT (B3LYP/6-31G**) methods show that the lysine substituent in the model diphosphate zwitterionic form retain similar orientation as observed in Fig. 2. The ribose phosphate backbone also retains torsion angles similar to the tRNA model of wobble nucleotide [44]. The phase angle of pseudorotation (P) and amplitude (Tm) of ribose ring of zwitterionic form of lysidine are calculated (Table 5) by using geometry optimized torsion angle values (T_1 , T_2 , T_3 , T_4 and T_5) of RM1, HF-SCF and DFT methods. The (P) and (Tm) values are calculated according to [56] and compared with the crystal structure values [44]. The results of P and Tm show some differences from the accepted range ($0-36^\circ$ for P and $35-45^\circ$ for Tm) for the $c3'$ -endo sugar conformation as given in [56]. So the pseudorotation value (P) falls within the range of (11.4 to 15.4°) and (Tm) value in the range of (26.8 to 40.4°) for the zwitterionic diphosphate form of lysidine. Hence, zwitterionic form of lysidine may be helpful in maintaining $c3'$ -endo sugar conformation to some extent at 34^{th} nucleotide position and prevents mismatch base pairing with G.

Diphosphate cytidine nucleotide

The conformational study of 5'-3' diphosphate nucleotide segment of cytidine (Fig. 3) is performed by PCILO method to compare the phosphate backbone of various diphosphate nucleotide forms of lysidine. The variations around the glycosyl torsion angle freely over the entire range ($0-360^\circ$) preferred ($\chi=33^\circ$) instead of ($\chi=3^\circ$) as observed in Figure 2. This small change in glycosyl torsion angle ($\chi=33^\circ$) results in strong hydrogen bonding (Table 1) between $O5'$ --- $HC(6)$ and weakens the interaction between $O1'$ --- $HC(6)$. The atom $HC(6)$ of cytidine is involved in bifurcative hydrogen bonding with $O5'$ and $O1'$ of phosphate backbone (Fig. 3). The interaction between $O1P_{b(35)}$ --- $HC3'$ may be the additional stabilizing factor for this conformation (Fig. 3).

The results of full geometry optimization of PCILO most stable conformation (Fig. 3) by HF-SCF (STO3G) are ($\chi=29^\circ$, $\zeta_{b(33)}=181^\circ$, $\alpha_{b(34)}=$

262° , $\beta_{b(34)}=158^\circ$, $\gamma_{b(34)}=201^\circ$, $\delta_{b(34)}=55^\circ$, $\epsilon_{b(34)}=89^\circ$, $\zeta_{b(34)}=206^\circ$, $\alpha_{b(35)}=317^\circ$, $\beta_{b(35)}=212^\circ$, $\gamma_{b(35)}=171^\circ$). The torsion angles χ , $\zeta_{b(33)}$, $\beta_{b(34)}$, $\delta_{b(34)}$, $\epsilon_{b(34)}$, $\zeta_{b(34)}$, $\beta_{b(35)}$ and $\gamma_{b(35)}$ differ to some minor extent whereas torsion angles $\alpha_{b(34)}$, $\gamma_{b(34)}$, differ by 40° and torsion angles $\alpha_{b(35)}$ show large variations as compared to Figure 3. Automated full geometry optimization of the PCILO preferred most stable conformation (Fig. 3) using RM1 method are ($\chi=0^\circ$, $\zeta_{b(33)}=223^\circ$, $\alpha_{b(34)}=246^\circ$, $\beta_{b(34)}=117^\circ$, $\gamma_{b(34)}=175^\circ$, $\delta_{b(34)}=51^\circ$, $\epsilon_{b(34)}=98^\circ$, $\zeta_{b(34)}=218^\circ$, $\alpha_{b(35)}=302^\circ$, $\beta_{b(35)}=267^\circ$, $\gamma_{b(35)}=207^\circ$). The torsion angles $\gamma_{b(34)}$, $\delta_{b(34)}$, $\zeta_{b(34)}$, and $\alpha_{b(35)}$, $\gamma_{b(35)}$ vary within 30° , whereas torsion angles $\zeta_{b(33)}$, $\alpha_{b(34)}$, $\beta_{b(34)}$, and $\beta_{b(35)}$ show large variation as compared to Figure 3. The results of full geometry optimization using the DFT (B3LYP/6-31G**) are ($\chi=11^\circ$, $\zeta_{b(33)}=174^\circ$, $\alpha_{b(34)}=266^\circ$, $\beta_{b(34)}=177^\circ$, $\gamma_{b(34)}=223^\circ$, $\delta_{b(34)}=54^\circ$, $\epsilon_{b(34)}=75^\circ$, $\zeta_{b(34)}=217^\circ$, $\alpha_{b(35)}=296^\circ$, $\beta_{b(35)}=192^\circ$, $\gamma_{b(35)}=168^\circ$). The minor differences observed in torsion angles χ , $\zeta_{b(33)}$, $\beta_{b(34)}$ and $\beta_{b(35)}$. The torsion angle $\delta_{b(34)}$, $\epsilon_{b(34)}$, $\gamma_{b(35)}$ changes by about 20° whereas the $\alpha_{b(34)}$, $\zeta_{b(34)}$ and $\alpha_{b(35)}$ differ by about 30° . The $\gamma_{b(34)}$ torsion angle changes to some large extent. The intra molecular interactions after the geometry optimization are shown in (Table 4). The results of geometry optimization by RM1, HF-SCF, DFT methods retain phosphate backbone values similar to crystal structure [44]. However, the geometry optimized methods HF-SCF and DFT also support the change in glycosyl torsion angle within the range of ($\chi=11^\circ$ to 29°) as predicted by PCILO method (Fig. 3) except RM1 method.

Geometry optimized values of (T_1 , T_2 , T_3 , T_4 and T_5) are used for the calculation of the phase angle of pseudorotation (P) and amplitude (Tm) (Table 5). The (P) value ranges from (24.0 to 44.9°) whereas amplitude (Tm) falls within the range of (22.6 to 41.6°) for the ribose ring of diphosphate cytidine nucleotide (Fig. 3). The higher (P) value range could be because of change in glycosyl torsion angle ($\chi=11^\circ$ to 29°) which could deviate $c3'$ -endo sugar conformation towards the $c2'$ -endo in (Fig. 3) as discussed in [44]. This change in glycosyl torsion angle (Fig. 3) may be because of absence of lysine substituent at C(2) position of cytidine with respect to all four forms of lysidine diphosphate nucleotides (Fig. 2, 4, 5 and 6) which maintains glycosyl torsion angle anti ($\chi=3^\circ$) conformation.

Diphosphate non-zwitterionic form of lysidine:

Figure 4 depicts the PCILO predicted most stable conformation for the 5'-3' diphosphate nucleotide segment of non-zwitterionic form of lysidine (Me- p - $k^2C_{(non-zwitterionic)}$ - p -Me). The preferred torsion angle values describing the base substituent and backbone orientation in non-

zwitterionic form of lysidine are

($\alpha=180^\circ$, $\beta=180^\circ$, $\gamma=30^\circ$, $\delta=60^\circ$, $\psi=180^\circ$, $\phi=60^\circ$, $\xi=30^\circ$, $\theta=180^\circ$, $\eta=180^\circ$, $\chi=3^\circ$). The lysine side chain folds back toward the ribose sugar ring, which results in formation of hydrogen bonding between the O2'H ---O(12a), O(12a)---HN(2), O(12a)---HC(9), N(2)---HC(9), N(2)---HC(10) and O(12b)---HN(11) (Table 1). The glycosyl torsion angle remains the choice of initial torsion angle ($\chi=3^\circ$) whereas, conformation of lysine substituent is similar to Figure 2. The structure is stabilized by interactions (Table 1) between O1'---HC(6), O5'---HC3' and O1P_{b(35)}---HC3' as found in Figure 2. The atom HC3' forms bifurcative hydrogen bonding with O1P_{b(35)} and O5' of ribose. The orientation of lysine substituent is found trans to the N(1) of cytidine in case of model diphosphate (Me-p-k²C_(non-zwitter)-p-Me) nucleotide segment of non-zwitterionic form of lysidine as compared with earlier results [31]. The amino and carboxyl groups of lysine substituent do not interact with 5' or 3' phosphate backbone.

The full geometry optimization have been carried out and the results are compared with the PCILO most structure of lysine substituent (Fig. 4) and crystal structure [44] for the phosphate backbone. The geometry optimized results by using semi-empirical quantum chemical RM1 method is

($\alpha=176^\circ$, $\beta=79^\circ$, $\gamma=55^\circ$, $\delta=65^\circ$, $\psi=185^\circ$, $\phi=71^\circ$, $\xi=309^\circ$, $\theta=184^\circ$, $\eta=182^\circ$, $\chi=12^\circ$, $\zeta_{b(33)}=222^\circ$, $\alpha_{b(34)}=241^\circ$, $\beta_{b(34)}=198^\circ$, $\gamma_{b(34)}=213^\circ$, $\delta_{b(34)}=47^\circ$, $\epsilon_{b(34)}=92^\circ$, $\zeta_{b(34)}=223^\circ$, $\alpha_{b(35)}=283^\circ$, $\beta_{b(35)}=163^\circ$, $\gamma_{b(35)}=183^\circ$). The torsion angles α , γ , δ , ψ , ϕ , θ , η , χ , $\beta_{b(34)}$, $\delta_{b(34)}$, $\epsilon_{b(34)}$, $\zeta_{b(34)}$ and $\alpha_{b(35)}$ show minor differences within 30°.

Whereas, torsion angles β , ξ , $\zeta_{b(33)}$, $\alpha_{b(34)}$, $\gamma_{b(34)}$ and $\beta_{b(35)}$ show some large variations. The geometry optimized results by using HF-SCF (STO-3G) results in torsion angle values

($\alpha=173^\circ$, $\beta=90^\circ$, $\gamma=54^\circ$, $\delta=63^\circ$, $\psi=203^\circ$, $\phi=67^\circ$, $\xi=62^\circ$, $\theta=180^\circ$, $\eta=182^\circ$, $\chi=27^\circ$, $\zeta_{b(33)}=177^\circ$, $\alpha_{b(34)}=184^\circ$, $\beta_{b(34)}=173^\circ$, $\gamma_{b(34)}=229^\circ$, $\delta_{b(34)}=55^\circ$, $\epsilon_{b(34)}=81^\circ$, $\zeta_{b(34)}=216^\circ$, $\alpha_{b(35)}=294^\circ$, $\beta_{b(35)}=261^\circ$, $\gamma_{b(35)}=193^\circ$). The torsion angles γ , ψ , χ , $\zeta_{b(34)}$ and $\alpha_{b(35)}$ vary by 30° whereas, the other torsion angles β , $\alpha_{b(34)}$, $\gamma_{b(34)}$ and $\beta_{b(35)}$ show some large difference. The other torsion angle show minor variations as compared to the PCILO preferred structure (Fig. 4).

The full geometry optimization using the DFT (B3LYP/6-31G**) results in the torsion angle value ($\alpha=174^\circ$, $\beta=129^\circ$, $\gamma=57^\circ$, $\delta=58^\circ$, $\psi=197^\circ$, $\phi=68^\circ$, $\xi=57^\circ$, $\theta=178^\circ$, $\eta=183^\circ$, $\chi=11^\circ$, $\zeta_{b(33)}=189^\circ$, $\alpha_{b(34)}=289^\circ$, $\beta_{b(34)}=148^\circ$, $\gamma_{b(34)}=162^\circ$, $\delta_{b(34)}=48^\circ$, $\epsilon_{b(34)}=81^\circ$, $\zeta_{b(34)}=196^\circ$, $\alpha_{b(35)}=303^\circ$, $\beta_{b(35)}=272^\circ$, $\gamma_{b(35)}=198^\circ$). The torsion angles α , δ , ϕ , ψ , θ , η , χ , $\zeta_{b(33)}$, $\alpha_{b(34)}$, $\gamma_{b(34)}$, $\delta_{b(34)}$, $\epsilon_{b(34)}$ and $\zeta_{b(34)}$ changes at minor differences from the PCILO preferred

conformation while the torsion angle γ , ξ , $\beta_{b(34)}$ and $\alpha_{b(35)}$ changes by about 30° while other torsion angle changes at large differences. The hydrogen bonding interactions after the geometry optimization by above discussed methods show similar results as found by PCILO method and are shown in (Table 4). This form of lysidine cannot form Watson-Crick base pairing with 'A' due to because trans orientation of N(2)H. Similarly, due to mismatch of proper hydrogen bond donor and acceptor groups and steric clashes with lysine substituent it cannot recognize 'G'.

The calculations of phase angle of pseudorotation (P) and amplitude (Tm) carried out by using the optimized torsion angle values of (τ_1 , τ_2 , τ_3 , τ_4 and τ_5) obtained by RM1, HF-SCF and DFT methods (Table 5). The (P) value differ within the range of (7.6 to 29.4°) and (Tm) value ranges from (29.3 to 39.5°) and found in the accepted range as shown in [56]. Results of glycosyl torsion angle (χ), pseudorotation value (P) and amplitude (Tm) indicates that non-zwitterionic form of lysidine may also support certain kind of structural stability at 34th position in anticodon loop of tRNA.

Diphosphate neutral form of lysidine:

The PCILO predicted most stable structure of 5'-3' diphosphate nucleotide segment of neutral form of lysidine (Me-p-k²C_(neutral)-p-Me) shown in Figure 5. The preferred torsion angle values describing the lysine substituent are

($\alpha=180^\circ$, $\beta=180^\circ$, $\gamma=30^\circ$, $\delta=60^\circ$, $\psi=180^\circ$, $\phi=60^\circ$, $\xi=30^\circ$, $\theta=150^\circ$, $\eta=180^\circ$, $\chi=3^\circ$). The lysine substituent and glycosyl torsion angle of the nucleotide diphosphate neutral form of lysidine (Fig. 5) show the similar kind of orientation as observed in Figure 2 and Figure 5. The lysine substituent folds back towards the ribose sugar and interacts with O(12a)---HO2', O(12a)---HN(2), O(12a)---HC(9), N(2)---HC(10) and O(12b)---HN(11) and shown in (Table 1). These results may be compared with earlier data [31]. The variations around the glycosyl torsion angle retain original value ($\chi=3^\circ$) as observed for the 34th nucleotide base in the crystal structure [44]. The structure is stabilized by interactions between O5'---HC(6), O5'---HC3', O1P_{b(35)}---HC3' and O1'---HC(6) similar to (Fig. 2 and 4). The interaction between carboxyl and amino groups of lysine moiety with 5' or 3' phosphate backbone is also not possible in diphosphate neutral lysidine.

The geometry optimized values by HF-SCF (STO-3G) method are ($\alpha=171^\circ$, $\beta=152^\circ$, $\gamma=53^\circ$, $\delta=61^\circ$, $\psi=192^\circ$, $\phi=67^\circ$, $\xi=63^\circ$, $\theta=184^\circ$, $\eta=181^\circ$, $\chi=5^\circ$, $\zeta_{b(33)}=190^\circ$, $\alpha_{b(34)}=296^\circ$, $\beta_{b(34)}=174^\circ$, $\gamma_{b(34)}=233^\circ$, $\delta_{b(34)}=53^\circ$, $\epsilon_{b(34)}=79^\circ$, $\zeta_{b(34)}=211^\circ$, $\alpha_{b(35)}=302^\circ$, $\beta_{b(35)}=271^\circ$, $\gamma_{b(35)}=191^\circ$). The optimized torsion angles α , δ , ϕ , η , χ , $\zeta_{b(33)}$, $\alpha_{b(34)}$ and $\beta_{b(34)}$ are similar by

($\pm 10^\circ$) from the PCILO stable structure (Fig. 5). Torsion angles γ , ψ , $\delta_{b(34)}$, $\epsilon_{b(34)}$, $\zeta_{b(34)}$ and $\gamma_{b(35)}$ are similar by ($\pm 20^\circ$) whereas other dihedral angles vary at some large extent. The full geometry optimization using the DFT (B3LYP / 6-31G**) methods results into ($\alpha=178^\circ, \beta=76^\circ, \gamma=54^\circ, \delta=67^\circ, \psi=207^\circ, \phi=66^\circ, \xi=52^\circ, \theta=212^\circ, \eta=176^\circ, \chi=16^\circ, \zeta_{b(33)}=203^\circ, \alpha_{b(34)}=281^\circ, \beta_{b(34)}=178^\circ, \gamma_{b(34)}=233^\circ, \delta_{b(34)}=53^\circ, \epsilon_{b(34)}=78^\circ, \zeta_{b(34)}=207^\circ, \alpha_{b(35)}=297^\circ, \beta_{b(35)}=190^\circ, \gamma_{b(35)}=166^\circ$). The torsion angles α , δ , ϕ , θ , η , $\beta_{b(34)}$ and $\beta_{b(35)}$ values are slightly differ from the PCILO preferred values whereas, the torsion angle χ , $\alpha_{b(34)}$, $\delta_{b(34)}$, $\epsilon_{b(34)}$, $\zeta_{b(34)}$, and $\beta_{b(35)}$ change by about 20° , the torsional γ , ψ , ξ , $\zeta_{b(33)}$ and $\alpha_{b(35)}$ changes by about 30° while, other torsional angle β , θ and $\gamma_{b(35)}$ changes by large differences. Optimized geometrical parameters are included in (Table 4). Neutral form of diphosphate lysidine may not allow recognizing 'A' due to because of trans orientation of lysine moiety as discussed in detail in our earlier study [31].

The geometry optimized torsion angle values (T_1 , T_2 , T_3 , T_4 and T_5) are considered for the calculation of phase angle of pseudorotation (P) and amplitude (Tm) (Table 4). The (P) and (Tm) values change within the range of (6.6 to 30.1°) and (16.2 to 42.4°) respectively and found appropriate in comparison with standard values [56]. Hence, by looking at glycosyl torsion angle, pseudorotation and amplitude values it clearly indicates that neutral form of lysidine diphosphate nucleotide maintains structural stability at 34th anticodon position. But this form of lysidine also cannot recognize 'A'. Hence, it is of interest to identify how tautomer form of lysidine maintains proper sugar conformation along with suitable hydrogen bond donor and acceptor groups to recognize 'A' and not 'G'.

Diphosphate tautomer form of lysidine:

Figure 6 describes the PCILO predicted most stable structure of 5'-3' diphosphate hypermodified nucleotide segment of tautomer form of lysidine (Me-p-k²C_(tautomer)-p-Me).

The preferred torsion angle values describing the base substituent orientation are ($\alpha=180^\circ, \beta=180^\circ, \gamma=30^\circ, \delta=210^\circ, \psi=150^\circ, \phi=0^\circ, \xi=0^\circ, \theta=300^\circ, \chi=3^\circ$). The lysine substituent folds back towards the 2'-hydroxyl group of ribose sugar ring. The structure is stabilized by hydrogen bonding interactions (Table 1) between the O2'H-----O(12b), O(12b)-----HN(2), O(12b)-----HC(9), O(12a)-----HN(11) and N(2)-----HC(9). The flipping of torsion angle θ to 300° and ψ to 150° resulted in strong interaction of 2'-hydroxyl group of ribose sugar with O(12b) instead of O(12a) of lysine substituent as compared to our earlier results [31]. These results (Fig. 6) may also be compared with zwitterionic (Fig. 2), non-

zwitterionic (Fig. 4), and neutral (Fig. 5) diphosphate lysidine forms (Table 1). This could be the minor effect of 3' -phosphate backbone on the carboxyl group of lysine substituent of tautomer form of lysidine as compared to earlier results [31]. After rotating freely the glycosyl torsion angle retains the original value ($\chi=3^\circ$) as in tRNA crystal structure [44]. The most stable structure (Fig. 6) is also stabilized by interactions between base and phosphate backbone O5'-----HC(6), O5'-----HC3', O1P_{b(35)}-----HC3' and O1'-----HC(6) similar to (Fig. 2, 4 and 5 and shown in Table 1). The lysine substituent of diphosphate tautomer form of lysidine also does not interact with 5' or 3' phosphate backbone as observed in zwitterionic, non-zwitterionic and neutral forms of lysidine.

Higher energy alternative (4.5 kcal/mol) conformation (Fig. 7) arrived by the flipping of the $\theta=120^\circ$ the interactions between O(12a)-----O2'H, O(12a)-----HC(9), and O(12a)-----HN(2) (Table 3) provides stability to the structure instead of O(12b) as observed in the most stable conformation (Fig. 6). The interaction between O1'-----HC(6), O5'-----HC3', O1P_{b(35)}-----HC3' and O5'-----HC(6) remains the stabilizing factor in the most stable and alternative most stable structures (Fig. 2-7).

The full geometry optimization of the PCILO most stable structure using the semi-empirical RM1 method results in

($\alpha=186^\circ, \beta=174^\circ, \gamma=77^\circ, \delta=210^\circ, \psi=117^\circ, \phi=314^\circ,$

$\xi=330^\circ, \theta=329^\circ, \chi=5^\circ, \zeta_{b(33)}=217^\circ, \alpha_{b(34)}=245^\circ, \beta_{b(34)}=206^\circ, \gamma_{b(34)}=217^\circ, \delta_{b(34)}=40^\circ, \epsilon_{b(34)}=86^\circ, \zeta_{b(34)}=206^\circ, \alpha_{b(35)}=301^\circ, \beta_{b(35)}=215^\circ, \gamma_{b(35)}=258^\circ$). The torsion angles α , β , δ , χ , $\delta_{b(34)}$, $\epsilon_{b(34)}$, $\zeta_{b(34)}$ and $\beta_{b(35)}$ show minor variations whereas, other torsion angles γ , ψ , ϕ , ξ , θ , $\zeta_{b(33)}$, $\alpha_{b(34)}$, $\beta_{b(34)}$, $\gamma_{b(34)}$, $\alpha_{b(35)}$ and $\gamma_{b(35)}$ show some differences from the PCILO preferred structure (Fig. 6). The optimization using the HF-SCF method yields

($\alpha=183^\circ, \beta=177^\circ, \gamma=76^\circ, \delta=212^\circ, \psi=102^\circ, \phi=325^\circ, \xi=344^\circ, \theta=316^\circ, \chi=28^\circ, \zeta_{b(33)}=189^\circ, \alpha_{b(34)}=258^\circ, \beta_{b(34)}=167^\circ, \gamma_{b(34)}=190^\circ, \delta_{b(34)}=58^\circ, \epsilon_{b(34)}=90^\circ, \zeta_{b(34)}=202^\circ, \alpha_{b(35)}=311^\circ, \beta_{b(35)}=258^\circ, \gamma_{b(35)}=192^\circ$).

The optimized torsion α , β , δ , θ , ϕ , ξ , χ , $\zeta_{b(33)}$, $\beta_{b(34)}$, $\delta_{b(34)}$, $\epsilon_{b(34)}$, $\zeta_{b(34)}$, $\beta_{b(35)}$ and $\gamma_{b(35)}$ are similar by ($\pm 20^\circ$) as compared to PCILO preferred structure (Fig. 6). The optimized values of the torsion angle γ , ψ and $\alpha_{b(35)}$ changes by $\pm 50^\circ$, $\alpha_{b(34)}$ differ by 39° and $\beta_{b(35)}$ vary by 59° . The full geometry optimization using the DFT (B3LYP / 6-31G**) methods results

into ($\alpha=183^\circ, \beta=183^\circ, \gamma=74^\circ, \delta=208^\circ, \psi=110^\circ, \phi=315^\circ, \xi=337^\circ, \theta=320^\circ, \chi=12^\circ, \zeta_{b(33)}=191^\circ, \alpha_{b(34)}=287^\circ, \beta_{b(34)}=149^\circ, \gamma_{b(34)}=162^\circ,$

$\delta_{b(34)}=46^\circ, \epsilon_{b(34)}=80^\circ, \zeta_{b(34)}=192^\circ, \alpha_{b(35)}=298^\circ, \beta_{b(35)}=275^\circ, \gamma_{b(35)}=195^\circ$). The torsion angles values for the the α , β , δ , χ , $\zeta_{b(33)}$, $\alpha_{b(34)}$, $\gamma_{b(34)}$,

$\epsilon_{b(34)}$, $\delta_{b(34)}$ and $\gamma_{b(35)}$ shows similar results as compared to the PCILO preferred values (Fig. 6). The torsion angle ξ , θ , $\beta_{b(34)}$ and $\alpha_{b(35)}$ change by about 30° whereas other torsion angle show large differences. The hydrogen bonding interactions obtained after the geometry optimization are shown in Table 5 and found similar to PCILO preferred conformation (Fig. 6).

The phase angle of pseudorotation (P) and amplitude (Tm) are calculated from the optimized values (T_1 , T_2 , T_3 , T_4 and T_5) obtained by RM1, HF-SCF and DFT methods (Table 5). The (P) value found within the range of (8.5 to 18.0) and (Tm) value observed within the range of (29.4 to 40). The pseudorotation (P) and amplitude (Tm) values for the zwitterionic, non-zwitterionic, neutral diphosphate nucleotides of lysidine and cytidine nucleotide differ to some extent than the crystal structure values [44]. Only the tautomer form of diphosphate nucleotide lysidine (Fig. 6) show less difference in (P) and (Tm) values (Table 5) as compared to the values of 34th nucleotide ribose sugar in tRNA model [44]. This may be because of the strong interaction of O(12b) of lysine substituent of tautomer form of lysidine (Fig. 6) with that of 2'-hydroxyl group of ribose sugar as compared to zwitterionic (Fig. 2), non-zwitterionic (Fig. 4), and neutral (Fig. 5) forms of lysidine. So tautomer form of lysidine may maintain the c3'-endo sugar puckering strongly as compared to the other forms of lysidine. But only tautomer form has got the proper hydrogen bond donor-acceptor groups at N(3) and N(4) sites respectively to form Watson-Crick hydrogen bonding with 'A' as compared to neutral form of lysidine as shown in earlier model [31].

Conclusion

In presence of 5'-3'diphosphate backbone the lysine substituent of various forms of lysidine interacts with the 2'-hydroxyl group of ribose sugar and prefers *trans* position with respect to N(1) of cytidine. Hence, the possibility of interaction of the amino and carboxyl groups of lysine substituent with 5' or 3' phosphate backbone is ruled out. Diphosphate cytidine nucleotide (Fig. 3) prefers ($\chi=33^\circ$), this change in glycosyl torsion angle could destabilize the c3'-endo sugar to c2'-endo sugar to some extent as discussed in tRNA model [44]. However, all the four forms of lysidine retain glycosyl torsion angle to its original value ($\chi=3^\circ$), which might help in maintaining the c3'-endo ribose sugar at 34th 'wobble' position. The results of hydrogen bonding parameters (Table 1), phase angle of pseudorotation (P) and amplitude (Tm) (Table 5) shows that the tautomer form of lysidine (Fig. 6) might help in stabilizing the c3'-endo sugar strongly as compared to the zwitterionic, non-zwitterionic and neutral forms of lysidine.

Hence, besides providing suitable hydrogen bond acceptor group at N(4), hydrogen bond donor group at N(3) and *trans* orientation of lysine substituent with respect to N(1) of cytidine, tautomer form of lysidine also provides suitable structural environment in the form of glycosyl orientation and ribose ring puckering in anticodon loop of tRNA for the recognition of AUA codons in place of AUG to avoid misrecognition of tRNA^{Met} instead of tRNA^{Ile}.

Acknowledgement: This work is supported by the Department of Science and Technology, Government of India, New Delhi through DST Fast Track project sanctioned to Dr. K.D.Sonawane is gratefully acknowledged.

References

- [1] Dunn D.B. (1959) *Biochimica et Biophysica Acta*, 34, 286-288.
- [2] Smith J.D. and Dunn D.B. (1959) *Journal of Biochemistry*, 72, 294-301.
- [3] McCloskey J.A. and Nishimura S. (1977) *Accounts of Chemical Research*, 10, 403-410.
- [4] Bjork G.R., Ericson J.U., Gustafsson C.E.D., Hagervall, T.G., Jonsson, Y.H., and Wikstrom P.M. (1987) *Annual Review of Biochemistry*, 56, 263-287.
- [5] Sprinzl M., Horn C., Brown M., Ludovitch, A. and Steinberg, S. (1998) *Nucleic Acids Research*, 26, 148-153.
- [6] Limbach P.A., Crain P.F. and McCloskey J.A. (1994) *Nucleic Acids Research*, 22, 2183-2196.
- [7] Persson B.C. (1993) *Molecular Microbiology*, 8, 1011-1016.
- [8] Agris P.F. (1996) *Progress in Nucleic Acid Research and Molecular Biology*, 53, 79-129.
- [9] Harada F. and Nishimura S. (1974) *Biochemistry*, 13, 300-307.
- [10] Kuchino Y., Watanabe S., Harada F. and Nishimura S. (1980) *Biochemistry*, 19, 2085-2089.
- [11] Andachi Y., Yamao F., Muto A. and Osawa S. (1989) *Journal of Molecular Biology*, 209, 37-54.
- [12] Matsugi J., Murao K. and Ishikura H.J. (1996) *J. of Biochemistry*, 119, 811-816.
- [13] Weber F., Dietrich A., Henry-Weil J. and Marechal-Drouard L. (1990) *Nucleic Acids Research*, 18, 5027-5030.
- [14] Gupta R. (1984) *Journal Biological Chemistry*, 259, 9461-9471.
- [15] Muramatsu T., Nishikawa K., Nemoto F., Kuchino Y., Nishimura S. Miyazawa T. and Yokoyama S. (1988) *Nature*, 336, 179-181.
- [16] Soma A., Ikeuchi Y., Kanemasa S., Kobayashi K., Ogasawara N., Ote T.,

- Kato J., Watanabe K., Sekine Y. and Suzuki T. (2003) *Molecular Cell*, 12, 689-698.
- [17] Grosjean H. and Bjork G.R. (2004) *Trends in Biochemical Sciences*, 29, 165-168.
- [18] Suzuki T. and Miyauchi K. (2010) *FEBS letters*, 584, 272-277.
- [19] Muramatsu T., Yokoyama S., Horie N., Matsuda A., Ueda T., Yamaizumi Z.,
- [20] Kuchino Y., Nishimura S. and Miyazawa T. (1988) *Journal of Biological Chemistry*, 263, 9261-9267.
- [21] Nakanishi K., Fukai S., Ikeuchi Y., Soma A., Sekine Y., Suzuki T. and Nureki O. (2005) *Proceedings of the National Academy of Sciences of the USA*, 102, 7487-7492.
- [22] Nakanishi K., Bonnefond L., Kimura S., Suzuki T., Ishitani R. and Nureki O. (2009) *Nature*, 461, 1144-1148.
- [23] Kuratani M., Yoshikawa Y., Bessho Y., Higashijima K., Ishii T., Shibata R., Seizo T., Yutani K. and Yokoyama S. (2007) *Structure*, 15, 1642-1653.
- [24] Ikeuchi Y., Kimura S., Numata T., Nakamura D., Takashi Y.T., Ogata T., Wada T., Suzuki T., Suzuki T. (2010) *Nature Chemical Biology*, 6, 277-282.
- [25] Tewari R. (1988) *International Journal of Quantum Chemistry*, 34, 133-142.
- [26] Sonawane K.D., Sonavane U.B. and Tewari R. (2002) *Journal of Biomolecular Structure Dynamics*, 19, 637-648.
- [27] Tewari R. (1987) *Indian J. of Biochemistry and Biophysics*, 24, 170-176.
- [28] Tewari R. (1990) *Journal of Biomolecular Structure Dynamics*, 8, 675-686.
- [29] Tewari R. (1995) *Chemical Physics Letters*, 238, 365-370.
- [30] Sonavane U.B., Sonawane K.D., Morin A., Grosjean H. and Tewari R. (1999) *Int. J. of Quantum Chemistry*, 75, 223-229.
- [31] Sonawane K.D., Sonavane U.B. and Tewari R. (2000) *International Journal of Quantum Chemistry*, 78, 398-405.
- [32] Sonawane K.D. and Tewari R. (2008) *Nucleosides Nucleotides and Nucleic Acids*, 27, 1158-1174.
- [33] Sonavane U.B., Sonawane K.D. and Tewari R. (2002) *Journal of Biomolecular Structure Dynamics*, 20, 473-485.
- [34] Sasisekharan V. and Lakshminarayanan A.V. (1969) *Biopolymers*, 8, 505-514.
- [35] Newton M.D. (1973) *Journal of American Chemical Society*, 95, 256-258.
- [36] Saran A. and Govil G. (1971) *Theoretical Biology*, 33, 407-418.
- [37] Pullman B., Perahia D. and Saran A. (1972) *Biochimica et Biophysica Acta*, 269, 1-14.
- [38] Tewari R., Nanda R.K. and Govil G. (1974) *Journal Theoretical Biology*, 46, 229-239.
- [39] Yathindra N. and Sundaralingam M. (1974) *Proceedings of the National Academy of Sciences of the USA*, 71, 3325-3328.
- [40] Matsuoka O., Tosi C. and Clementi E. (1978) *Biopolymers*, 17, 33-49.
- [41] Govil G. (1976) *Biopolymers*, 15, 2303-2307.
- [42] Tewari R., Nanda R.K. and Govil G. (1974) *Biopolymers*, 13, 2015-2035.
- [43] Watts M.T. and Tinoco I. (1978) *Biochemistry*, 17, 2455-2463.
- [44] Norman S.K., Holmes H.M., Stempel L.M. and Ts'o P.O.P. (1970) *Biochemistry*, 9, 3479-3498.
- [45] Holbrook S.R., Sussman J.L., Warrant R.W. and Kim S.H. (1978) *Journal of Molecular Biology*, 123, 631-660.
- [46] Diner S., Malrieu J.P. and Claverie P. (1969) *Theoretical Chimica Acta*, 13, 1-17.
- [47] Diner S., Malrieu J.P., Jordan, F. and Gilbert M. (1969) *Theoretical Chimica Acta*, 15, 100-110.
- [48] Malrieu J.P. (1977) *In Semiempirical Methods of Electronic Structure Calculations, Part A: Techniques; Segal, G.A., Ed.; Plenum: New York*, P. 69.
- [49] Pullman B. and Pullman A. (1974) *Advances in Protein Chemistry*, 16, 347-526.
- [50] Pullman B. and Saran A. (1976) *Progress in Nucleic Acid Research and Molecular Biology*, 18, 216-326.
- [51] Sharma S., Sonavane U.B. and Joshi R.R. (2009) *International Journal of Quantum Chemistry*, 109, 890-896.
- [52] Tewari R. (1987) *International Journal Quantum Chemistry*, 31, 611-624.
- [53] Rocha G.B., Freire R.O., Simas A.M. and Stewart J.P. (2006) *Journal Computational Chemistry*, 27, 1101-1111.
- [54] Becke A.D. (1993) *Journal of Chemical Physics*, 98, 5648-5652.
- [55] Francl M.M., Pietro W.J., Hehre W.J., Binkley J.S., Gordon M.S., Defrees D.J. and Pople J.A. (1982) *Journal of Chemical Physics*, 77, 3654-3665.
- [56] Hehre W.J., Radom L., Schleyer P.V.R., Pople J.A. (1986) *In Ab Initio Molecular Orbital Theory Wiley New York*.
- [57] Altona C. and Sundaralingam M. (1972) *Journal of American Chemical Society*, 94, 8205-8212.

Table 1- Hydrogen bonding parameters for the PCILO preferred conformations of 5'-3' diphosphate nucleotide segment of various lysidine forms.

Atoms involved	Distance	Distance	Angle	Fig.
(1-2-3)	atom pair	atom pair	1/2/2003	Ref
	1-2(A°)	2-3 (A°)	(Deg.)	
O(12a)----HO2'	1.68	0.95	172.42	2,5
O(12a)----HO2'	1.75	0.95	151.5	4
O(12a)----HN(2)	2.59	1	157.77	2,5
O(12a)----HN(2)	2.4	1	154	4
N(2)-----HC(9)	2.42	1	94.32	2,4,5
N(2)-----HC(9)	2.15	1	110.67	6
N(2)-----HC(10)	2.65	1	110.42	2,4,5
O(12a)----HC(9)	2.02	1	131.72	2,5
O(12a)----HC(9)	2.16	1	129.43	4
O(12b)----HN(11)	1.74	1	119.52	2,5
O(12b)----HN(11)	2.05	1	114.36	4
O(12b)----HC(9)	1.86	1	147.69	6
O(12b)----HO2'	1.43	0.95	152.5	6
O(12b)----HN(2)	2.05	1	163.51	6
O(12a)----HN(11)	1.64	1	123.24	6
O1'-----HC(6)	1.93	1	112.74	2,4,5,6
O1'-----HC(6)	2.14	1	105.09	3
O5'-----HC(6)	1.97	1	157.14	3
O5'-----HC(6)	2.64	1	118.15	2,5
O5'-----HC(6)	2.58	1	118.2	4,6
O5'-----HC3'	2.12	1	110.48	2,3,5,
O5'-----HC3'	2.09	1	110.54	4,6
O1Pb(35)----HC3'	2.33	1	104.13	2,3,5,
O1Pb(35)----HC3'	2.32	1	105.38	4,6

Table 2- Most stable and alternative stable conformations for the 5'-3' diphosphate nucleotide segments of various forms of lysidine.

Torsion angles	Rel. Energy	Fig. Ref.
1) Zwitterion form:		
a=180°, b=180°, g=30°, d=60°, y=180°, φ=60°, ξ= 330°, θ=150°, χ=3°.	0	2
2) Non-Zwitterionic form:		
a=180°, b=180°, g=30°, d=60°, y=180°, φ=60°, ξ=30°, θ=180°, η=180°, χ=3°.	0	4
3) Neutral Form :		
a=180°, b=180°, g=30°, d=60°, y=180°, φ=60°, ξ= 30°, θ=150°, η=180°, χ=3°.	0	5
4) Tautomer form:		
a=180°, b=180°, g=30°, d=210°, y=150°, φ=0°, ξ=0°, θ=300°, c=3°.	0	6
Alternative No 1:		
a=180°, b=180°, g=30°, d=210°, y=150°, φ=0°, ξ= 0°, θ=120°, c=3°.	4.5	7

Table 3- Hydrogen bonding -geometrical parameters for the alternative stable 5'-3' diphosphate nucleotide segments of various forms of the lysidine.

Atoms involved	Distance	Distance	Angle	Fig.
(1-2-3)	atom pair	atom pair	1/2/2003	Ref.
	1-2(A°)	2-3 (A°)	(Deg.)	
O(12a)---HO2'	1.34	0.96	148.47	
O(12a)---HN(2)	1.88	1	168.31	
N(2)-----HC(9)	2.15	1	110.67	
O(12a)---HC(9)	1.8	1	150.83	
O(12b)---HN(11)	1.8	1	117.21	7
O(12a)---HC1'	2.28	1	112.66	
O5'-----HC (6)	2.58	1	118.2	
O1'-----HC(6)	1.94	1	112.78	
O5'-----HC3'	2.09	1	110.54	

Table 4- Hydrogen bonding parameters obtained from the geometry optimization of PCILO preferred conformations by using the various methods

Method used	RM1		HF-SCF		DFT		Fig. Ref
Atom involved	r12	<123	r12	<123	r12	<123	
(1-2-3)							
O(12a)---HO2'	2.59	133.08	1.69	161.72	1.85	154.13	2
O(12a)---HN(2)	2.35	146.87	1.73	167.95	2.05	155.46	2
O1'-----HC(6)	2.27	99.11	2.33	95.67	2.26	100.23	2
O1'-----HC(6)	2.35	97.04	2.36	98.45	2.29	101.13	3
O5'-----HC(6)	3.00	125.50	2.17	166.70	2.86	146.32	3
O(12a)---HN(2)	1.77	127.29	1.68	165.39	1.81	171.41	4
O(12a)---HO2'	2.61	140.75	1.92	162.38	2.23	164.27	4
O1'-----HC(6)	2.33	96.93	2.28	98.32	2.18	104.01	4
O(12a)---HO2'	4.17	117.30	1.79	172.84	1.80	146.96	5
O(12a)---HN(2)	2.54	170.21	2.35	152.23	2.14	153.67	5
O1'-----HC(6)	2.36	96.86	2.16	105.02	2.25	102.04	5
O5'-----HC3'	2.48	100.41	2.54	102.90	2.53	101.87	5
O(12b)---HO2'	1.80	142.20	1.77	163.98	1.86	165.92	6
O(12b)---HN(2)	1.72	164.47	1.62	164.66	2.07	158.36	6
O1'-----HC(6)	2.26	100.64	2.27	100.26	2.19	104.58	6
O5'-----HC(6)	2.51	131.66	1.85	172.25	2.30	141.65	6

Table 5- Geometry optimized torsion angle values of ribose ring, phase angle of pseudorotation (P) and amplitude (T_m) of the 5'-3' diphosphate nucleotide segment of the various forms of lysidine and cytidine nucleotide

Molecules	Methods	τ_1	τ_2	τ_3	τ_4	τ_5	(P)	(T_m)
Zwitterion	RM1	4	-22	29	-28	16	11.4	29.6
	HF-SCF	3	-19	26	-27	15	14.0	26.8
	DFT	3	-26	39	-39	23	15.4	40.4
Cytidine	RM1	-10	-5	16	-23	21	44.9	22.6
	HF-SCF	-2	-17	27	-30	20	22.9	29.3
	DFT	-7	-18	35	-40	30	28.7	39.9
Non-Zwitterion	RM1	-5	-14	26	-31	23	29.4	29.8
	HF-SCF	2	-23	33	-35	21	17.0	34.5
	DFT	7	-29	39	-36	19	9.0	39.5
Neutral	RM1	-3	-8	14	-17	13	30.1	16.2
	HF-SCF	5	-27	36	-36	19	11.7	36.8
	DFT	2	-26	38	-38	22	15.3	39.4
Tautomer	RM1	7	-27	35	-33	17	8.5	35.4
	HF-SCF	1	-19	28	-30	18	18.0	29.4
	DFT	6	-29	39	-37	19	9.9	39.6

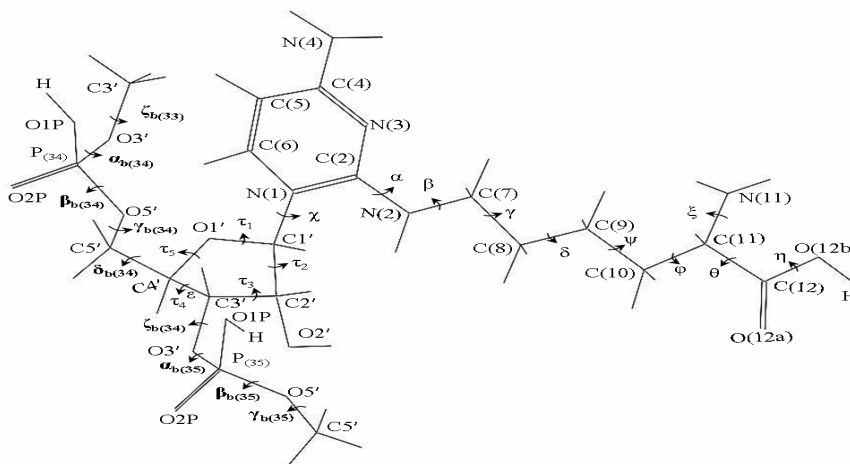


Fig. 1-Atom numbering and various torsion angles in model 5'-3' diphosphate nucleotide segment of lysidine (Non-Zwitterion form: Me-p-k²C_(non-zwit)-p-Me).

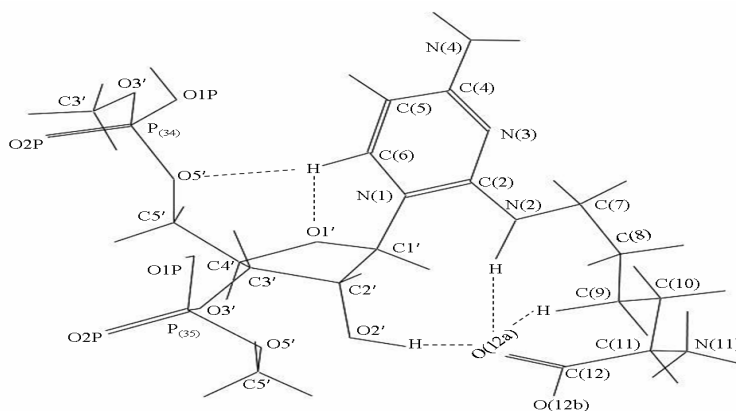


Fig. 2-PCILO predicted most stable structure of 5'-3' diphosphate hypermodified nucleotide segment of zwitterionic form of lysidine (Me-p-k²C_(zwit)-p-Me).

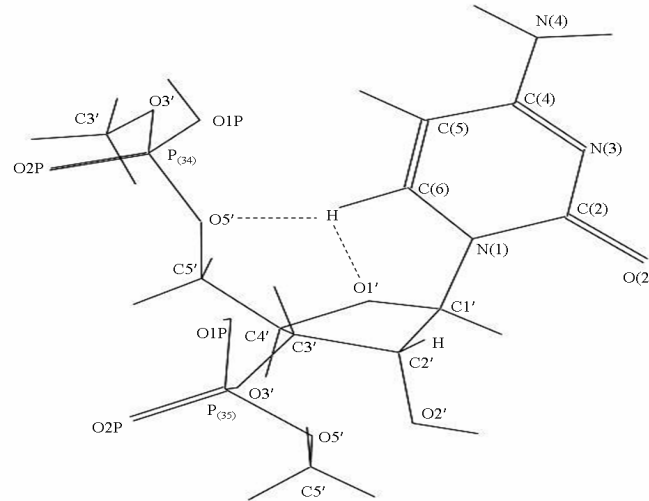


Fig. 3- PCILO predicted most stable structure of 5'-3' diphosphate cytidine nucleotide (Me-p-Cyt-p-Me).

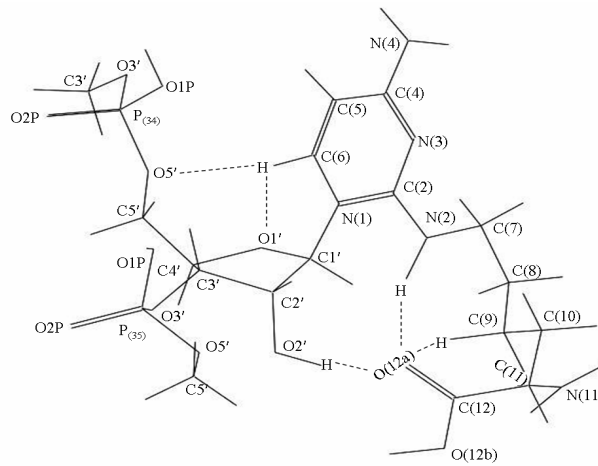


Fig. 4-PCILO predicted most stable structure of 5'-3' diphosphate hypermodified nucleotide segment of non-zwitterionic form of lysidine (Me-p-k²C_(non-zwit)-p-Me).

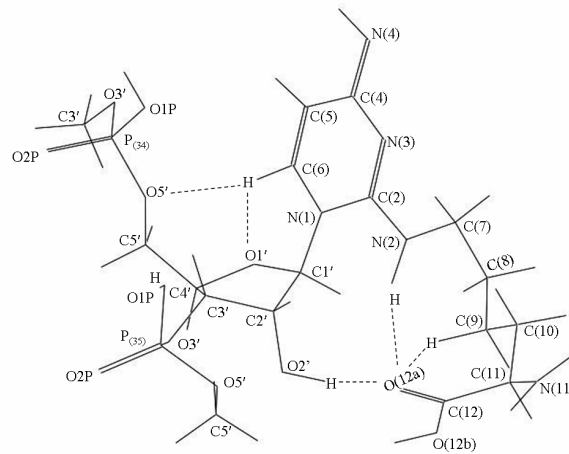


Fig. 5-PCILO predicted most stable structure of 5'-3' diphosphate hypermodified nucleotide segment of neutral form of lysidine (Me-p-k²C_(neutral)-p-Me).

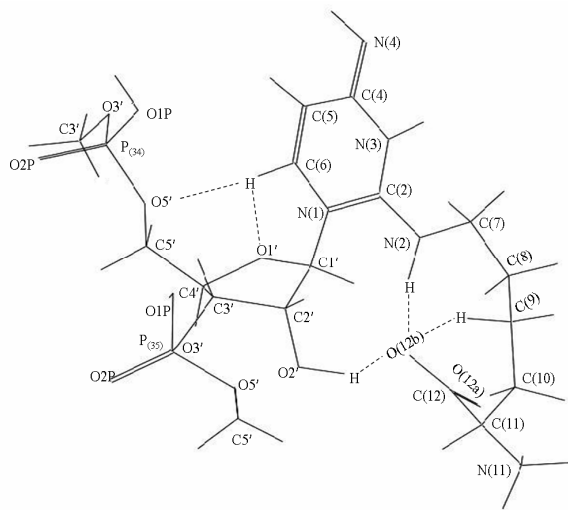


Fig. 6-PCILO predicted most stable structure of 5'-3' diphosphate hypermodified nucleotide segment of tautomer form of lysidine (Me-p-k²C_(taut)-p-Me).

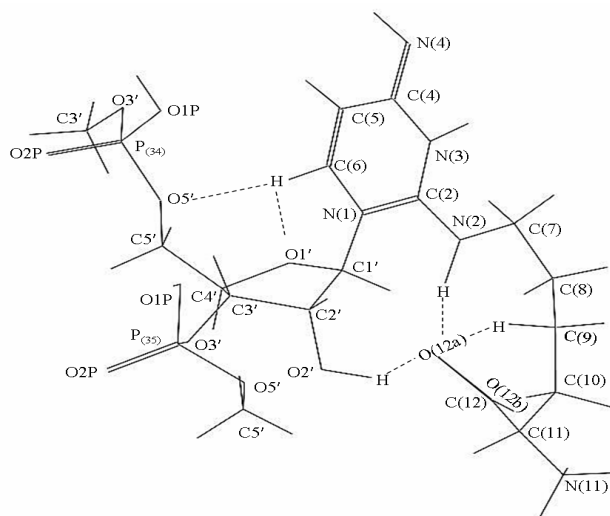


Fig. 7- Alternative structure for 5'-3' diphosphate hypermodified nucleotide segment of tautomeric (Me-p-k²C_(taut)-p-Me) form of lysidine ($\theta=120^\circ$).